Regular Article

PHYSICAL CHEMISTRY RESEARCH
Published by the
Iranian Chemical Society
www.physchemres.org
info@physchemres.org

Phys. Chem. Res., Vol. 12, No. 4, 935-947, December 2024
DOI: 10.22036/pcr.2024.447527.2493

Interaction of the Hydrochloroquine Drug with $B_{24}N_{24}$ Nanocage Doped by B, Al, and Si Elements: A Quantum Mechanical Simulation

Z. Javanshir[a,*], M. Razavi Mehr[b], M.H. Fekri[b] and V. Shekasteband[a]

[a]*Department of Chemistry, Faculty of Sciences, Ahar Branch, Islamic Azad University, Ahar, I.R. Iran*

[b]*Department of Chemistry, Faculty of Sciences, Ayatollah Boroujerdi University, Boroujerd, Iran*

(Received 8 March 2024, Accepted 2 July 2024)

Within the present work, the adsorption behavior of hydroxychloroquine drug onto $B_{24}N_{24}$ nanocage, and doped $B_{24}N_{24}$ nanocage with Si and Al has been investigated by B3LYP density functional at the 6-31G(d,p) level. To improve the interaction strength and drug adsorption on the $B_{24}N_{24}$ nanocage, we substituted a boron atom with aluminum and silicon. The electronic and geometric virtues in terms of adsorption arrangement, frontier molecular orbitals, adsorption energy, gap energy, chemical hardness, dipole moment, chemical potential, density of state (DOS), and the quantum theory of the atom in the molecule (QTAIM) analyses are calculated. Results showed that the negative absorption energy increased and the electronic properties of Al-doped BN were improved for drug absorption. Therefore, the study of the drug release mechanism indicates that in cells with a low pH, the tendency of the drug to release into the target cells increases.

Keywords: COVID-19, Hydroxychloroquine, Chemical potential, $B_{24}N_{24}$ nanocage, Drug release

INTRODUCTION

Currently, there is no definite and proven treatment for the disease caused by the coronavirus (Covid-19). From the beginning of this disease outbreak, hydroxychloroquine (HCQ) was proposed as an effective drug in the treatment of COVID-19 [1,2]. However, the role of hydroxychloroquine and its mechanism against the coronavirus have not yet been fully determined [3]. Due to its long half-life, HCQ may cause extensive secondary effects in the body or many drug interactions, such as retinopathy, hypoglycemia, and even cardiotoxicity. Using a powerful drug delivery system can reduce the side effects of this drug [4]. Therefore, it can provide greater safety in practice for its use in the treatment of COVID-19.

One of the important methods in drug delivery is the surface absorption method [5,6]. For this purpose, various adsorbents are used, the important condition of which is that they are not toxic [7]. The most important drug carriers that are used today can be mentioned as MCM-41, MCM-48, SBA-15, SBA-16, fullerene, and B_xN_x family [8-10]. 2D materials have garnered significant interest among the nanostructures applicable to drug delivery due to their ample surface area, facilitating the loading of numerous drug-a notable advantage in drug delivery applications [11-12]. Among the studies were conducted to use B_3O_3 nanosheets as a potential vehicle for TEPA drugs in the treatment of cancer tissues [13,14,15]. Also, the study has been conducted on the adsorption of chloroquine (CQ) and hydroxychloroquine (HCQ) on BC_3 nanosheets in gas and water environment, which demonstrated that BC_3 nanosheets, when hydrogenated, serve as more effective carriers for CQ and HCQ compared to single-layer BC3 [16,17,18]. In recent years, research has focused on using nanocarriers for drug delivery due to their low toxicity in the human body, so they can be used as nanocarriers in drug-release systems [19,20], simple synthesis, and high loading capacity of compounds [21].

Boron nitrides (B_xN_x) nanostructures are stable nanocages and tend to connect with other molecules due to

*Corresponding author. E-mail: za.javanshir@iau.ac.ir

the relatively strong ionic bond formed between nitrogen and boron atoms [22]. Previous research has shown that the electronic properties of these compounds change with the doping of boron atoms and that this affects their reactivity against other molecules [23,24].

Padish *et al.* studied the interactions of the sulfamide drug onto $X_{12}Y_{12}$ fullerene-like nanocages by the computational quantum mechanical method. They demonstrate that the sulfamide drug greatly altered the HOMO and LUMO energy levels upon adsorption on the examined nanocages, resulting in a reduction in the band gap values (E_g). Reducing the band gap increases the electrical conductivity of nanocages. These results indicate that the studied nanocages may be potential electronic sensors and also suitable candidates for sulfamide drug delivery in biological systems [25]. El-megeed *et al.* show the ability of $B_{12}N_{12}$ fullerene-like nanoclusters as a drug carrier for isoniazid anti-tuberculosis drugs has been studied by DFT methods [26]. Oku *et al.* successfully synthesized $B_{24}N_{24}$ fullerene [27]. Chen *et al.* demonstrated that nanostructures made of boron nitride (BN) are noncytotoxic and can be functionalized for use in biological contexts. Furthermore, they utilized BN nanotubes as a carrier for transporting DNA oligomers to the cells [28]. Suleimannejad *et al.* investigated the adsorption and release of the anticancer drug Aloe Emodin on $B_{24}N_{24}$ nanocages in gas and water phase. The interaction between nanocage and drug revealed that adsorption energies of the aloe-emodin drug on the $B_{24}N_{24}$ nanocage in the most stable complexes range from -0.87 to -0.75 eV in both gas phase and water. Binding of the drug to $B_{24}N_{24}$ also notably augmented the dipole moment of the drug carrier, desirable property for drug delivery within biological settings. The results of the study indicate that the $B_{24}N_{24}$ nanocages may be a potential carrier for the delivery of Aloe-Emodin drugs [29].

In this research, Gauss View software was used to design HCQ, pristine $B_{24}N_{24}$, and doped with Si-, B-, and Al-doped $B_{24}N_{24}$ and their complexes. The energies of the highest occupied and the lowest unoccupied molecular orbitals (HOMO & LUMO), gap energy (E_g), and general characteristics such as chemical potential (μ), chemical hardness (η), maximum charge transfer (ΔN_{max}), electrophilicity index (ω), *etc*. were calculated. Our other goal in this research is to investigate the use of a new series of nanocarriers in the controlled release of an effective drug against COVID-19 with the aim of reducing the side effects of the drug. The prospect of this work can help health researchers in the treatment of COVID-19 by conducting clinical research effectively.

COMPUTATIONAL DETAILS

Theoretical calculations including investigating the interactions of hydroxychloroquine drug with $B_{24}N_{24}$, $B_{23}AlN_{24}$, and $B_{23}SiN_{24}$ nanocages with the Gaussian 2009 program were performed [30]. The optimization of the various arrangements of pristine and complex forms of nanocages and drugs, the energy of the most stable structure, was studied by the B3LYP density functional of the 6-31G(d,p) basis set [31]. The following equation was used to calculate the adsorption energy between the nanocages and the drug hydroxychloroquine.

$$E_{ads} = [E_{complex}] - [E_{nanocage} + E_{hydroxychloroqine}] \quad (1)$$

Where E_{ads}, $E_{complex}$, $E_{nanocage}$, and $E_{hydroxychloroqine}$ represent the total energy adsorption, the energy of the hydroxychloroquine drug adsorbed with nanocages, the energy of nanocages alone and the energy of the hydroxychloroquine drug, respectively.

$$E_{cho} = \frac{E_{tot} - \sum_i n_i E_i}{j} \quad (2)$$

Where E_{tot}, n_i, and E_i are the entire energies of the drug-nanocage complexes, and the amount of particles sort i (i = H, O, C, Cl, N, B, Si, and Al), the atomic energy, respectively, and value j represents the overall number of atoms within the composition of drug-nanocage complexes. After optimizing the geometries, quantum mechanical descriptors were used to describe the electronic properties such as ionization potentials (I), electron affinity (A), chemical potential (μ) global hardness (η), electrophilicity index (ω), maximum charge transfer (ΔN_{max}), electronegativity (χ) and Fermi level (E_{FL}). These indexes were given by the following equations [32]:

$$E_g = E_{LUMO} - E_{HOMO} \quad (3)$$

$$\mu = -\frac{(I+A)}{2} \quad (4)$$

$$\eta = \frac{(I-A)}{2} \quad (5)$$

$$\omega = \frac{\mu^2}{2\eta} \quad (6)$$

$$\chi = -\mu \quad (7)$$

$$\Delta N_{max} = -\frac{\mu}{\eta} \quad (8)$$

$$E_{FL} = \frac{E_{LUMO}+E_{HOMO}}{2} \quad (9)$$

Furthermore, they were calculated to assess the plausibility of drug adsorption with the nanocage carriers [33,34]. The program GaussSum is used to get the density of states (DOS) plots [35]. The approach of the quantum theory of atoms in molecules (QTAIM) is valuable to get the amounts of electron density and bonding attributes of the configurations. Which uses AIM2000 software [36].

RESULTS AND DISCUSSIONS

The optimized geometry and electrostatic potential map (ESP) of hydroxychloroquine are presented in Fig. 1. Electrostatic potentials computed on the molecular surfaces of a single hydroxychloroquine drug showed that the N atom of the drug's aromatic ring and the O atoms of the drug might be taken into account as probable active sites when the connection with the $B_{24}N_{24}$ carrier is made (Fig. 1) [37-39]. Although the atoms of N (3) and N (4) have negative electrostatic potential, the nitrogen atom (3) probably cannot be the site of absorption due to steric effects [40]. Furthermore, the regions with the highest density of HOMO and LUMO profiles are mainly located on the N (5) and O atoms, respectively, which correspond to the blue and red areas on the ESP diagram. Since then, blue and red colors in the ESP map in order show over positive and negative areas, (Fig. 1) [41].

$B_{24}N_{24}$ is composed of 6 octagonal, 8 hexagonal, and 12 tetragonal rings. Three sorts of B-N bonds are recognized their bond lengths, in order, are about 1.47, 1.49, and 1.42 Å. In the same way, three sorts of B-N-B or N-B-N

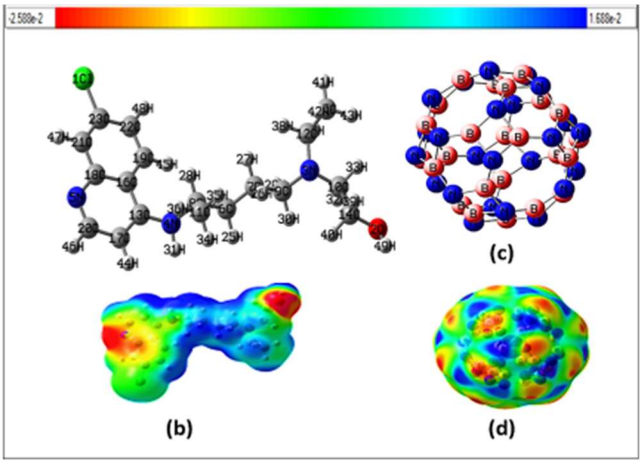

Fig. 1. Optimized structures of hydroxychloroquine drug (a), The ESP images of the drug (b), Optimized structure of $B_{24}N_{24}$ nanocage (c), The ESP image of $B_{24}N_{24}$ nanocage (d).

angles are recognized. The N-B-N angles are bigger than the related B-N-B ones. The amounts of NBN angles related to the hexagonal, octagonal, and tetragonal rings in order are around 122.8°, 136.2°, and 96.9°. The electrostatic potential map of $B_{24}N_{24}$ shows that primarily the boron in $B_{24}N_{24}$ wants to have an interaction with the oxygen and nitrogen atoms of the hydroxychloroquine drug (Fig. 1).

Optimization, Thermodynamic, and Electronic Properties of the Structures

The adsorption behavior of the hydroxychloroquine drug on the surface of $B_{24}N_{24}$ fullerene with optimized structures was investigated. For this reason, active sites including O, and N of the drug were selected to interact with the $B_{24}N_{24}$ fullerene from the direction of the B atom. Adsorption energy (E_{ad}) was calculated for all optimized complexes. Results showed that the boron and an N atom had a relatively strong middle bond, with E_{ad} = -19.53 kcal mol^{-1} (complex A), while the other O atom has an interaction with boron, with E_{ad} = -10.37 kcal mol^{-1} (complex B) (Table 2). In order to better understand the interaction between nanocage and hydroxychloroquine medication, the bond lengths between medicating and nanocarriers were calculated from optimized structures.

The bond lengths between optimized structures of the drug and nanocarriers were calculated to understand more

about the interaction between the nanocage and the hydroxychloroquine drug. According to the results, $B_{24}N_{24}$-N-Drug's (complex A) bond length with 1.645 Å and $B_{24}N_{24}$-O-Drug's (complex B) interaction distances are about 1.708 Å (Fig. 2). The value of NBN angles with an adsorbent boron atom (complex A) corresponding to the hexagonal, octagonal, and tetragonal rings, changes to 113.89°, 122.50°, and 90.41°, respectively. For complex B of numerical values in order around 116.8°, 127.3°, and 92.6°, respectively, it indicates a weaker interaction within complex B than complex A.

The electric dipole moment of $B_{24}N_{24}$ is calculated to be zero, and for the drug, the dipole moment value is 0.07 Debye and for complexes A and B, this value is around 15.72 and 4.96 Debye (Table 1). To improve the properties of the $B_{24}N_{24}$ carrier for drug absorption, an aluminum or silicon atom was replaced with a boron atom from the $B_{24}N_{24}$ nanocage. In the next step, hydroxychloroquine drug absorption was investigated with a doped $B_{24}N_{24}$ nanocage, it was considered that oxygen and nitrogen atoms of hydroxychloroquine interact with the Al and Si-doped atoms.

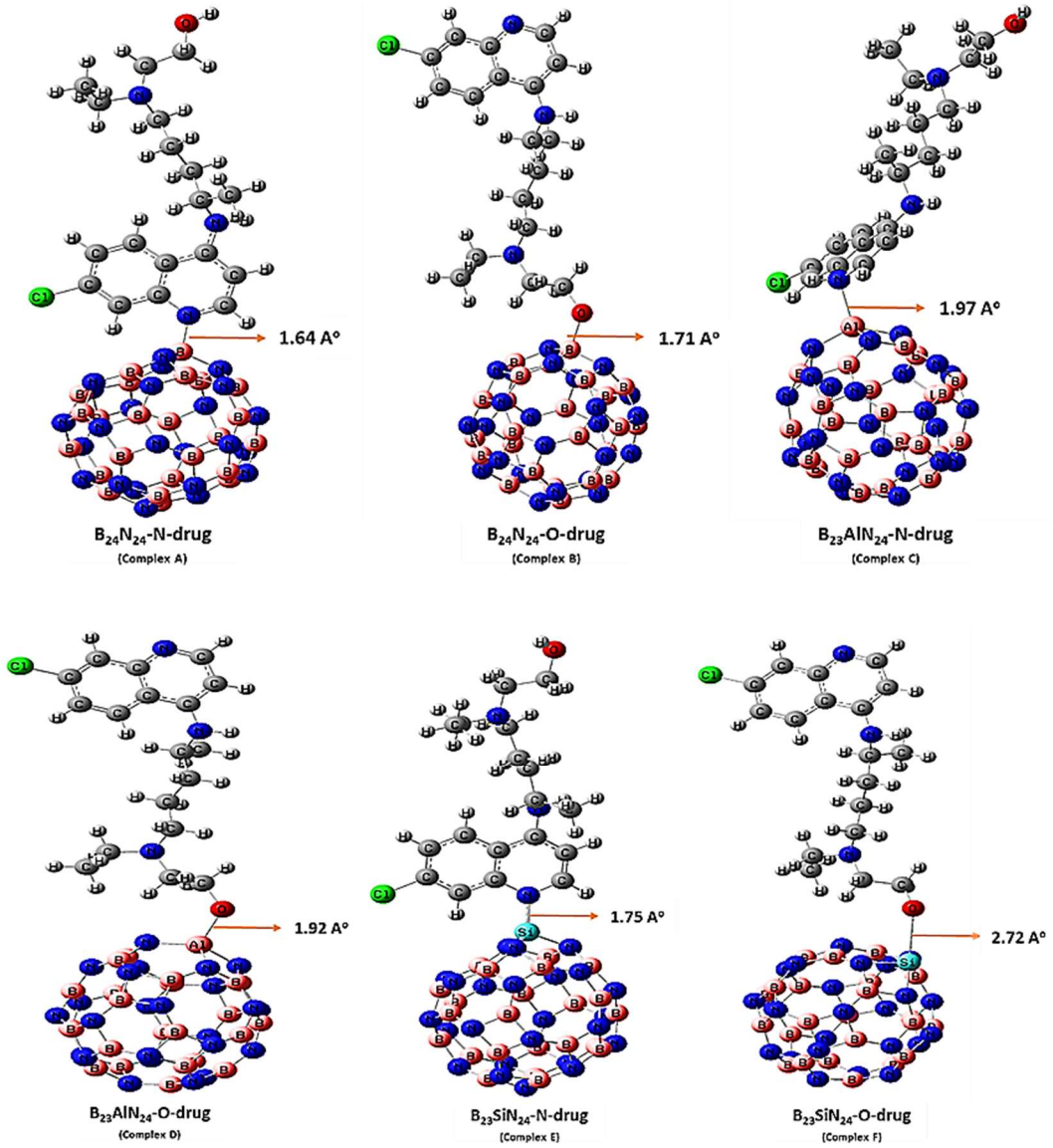

Fig. 2. Optimized structure of $B_{23}MN_{24}$-X-Drug (M = B, Si, and Al; X = N and O).

The optimized structures are shown in Fig. 2. In between all complexes, the $B_{23}AlN$-N-hetero drug (complex C) has the most stable structure, with an E_{ad} value = -49.09 kcal mol^{-1}. The N atom of the drug in complex C forms a chemical interaction with the Al atom, the bond length with 1.975 Å, and for $B_{23}AlN_{24}$-O- Drug (complex D), Ead decreases and is equal to -40.20 kcal mol^{-1} (Table 2). In complex D distance between O-Al bonds is about 1.917 Å. The results show that the doping of the aluminum atom significantly improves the interaction of the drug with the nanocage. Al-doping improves the drug delivery properties of nanocages. By doping the $B_{24}N_{24}$ with aluminum, the electric dipole moment increases. The dipole moment of $AlB_{23}N_{24}$ is calculated to be 2.66 Debye.

Similar calculations for Si-doped $B_{24}N_{24}$ fullerene were performed. The optimized structures have been shown in Fig. 2, and the results are in Table 3. The optimized structure of $B_{23}SiN_{24}$ (the Si atom) on the surface of the cage is projected out. The bond length of Si-N is about 1.72 Å. $B_{23}SiN_{24}$-N-hetero drug (complex E) with E_{ad} = -30.71 kcal mol^{-1} and for $B_{23}SiN_{24}$-O-drug (complex F) with the value of E_{ad} of -5.16 kcal mol^{-1} which in complex F, is a relatively lower negative value that can be due to the change in shape of the drug and nanocage after the interaction. Complex E with E_{ad} = -30.71 kcal mol^{-1} is the stable structure. For complex E, the nitrogen atom of the drug shapes a chemical interaction with Si, whereas the O atom of the drug contains a relatively weak interaction with Si atoms. The bond length for $B_{23}SiN_{24}$-N-Drug is 1.748 Å and for $B_{23}SiN_{24}$-O-Drug (complex F) is 2.722 Å.

The discrepancy in bond length between doped cage-drug can be related to the different N and O electronegativity of drug atoms and doped cage atoms. The dipole moment value for $B_{23}SiN_{24}$ is 0.82 Debye, and those for $B_{23}SiN_{24}$-N-hydroxychloroquine and $B_{23}SiN_{24}$-N-hydroxychloroquine complexes are about 2.43 and Debye. Due to the map of electrostatic potentials of $B_{24}N_{24}$ and the doped $B_{24}N_{24}$ nanocage, displayed in Fig. 3, the active sites related to $B_{23}AlN_{24}$ and $B_{23}SiN_{24}$ are the Al and Si atoms, respectively.

The diagram of HOMO and LUMO plots is shown in Fig. 4 and their E_g is given in Table 3. According to calculations, the value of E_g = 6.48 eV for the $B_{24}N_{24}$ nanocage was obtained. The E_g factor is a suitable factor for determining the active reactivity of materials; additionally, it

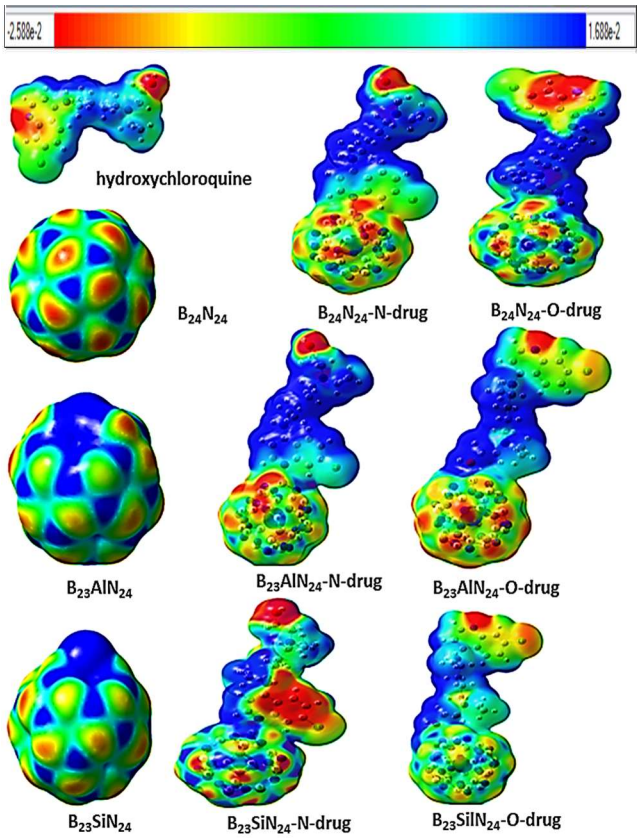

Fig. 3. The ESP images of drugs and drug nanocarriers.

alters upon the adsorption process, demonstrating the sensitivity of an adsorbent agent to an adsorbate material according to the taking condition. After the interaction of the nanocage with the drug, the LUMO of the nanocage has been moved onto the drug in all structures. Additionally, the diagram of DOS for $B_{24}N_{24}$ was recently updated, and after interaction with hydroxychloroquine, the drug is displayed in Fig. 5. The profiles of structures show that the LUMO level is considerably localized on the impurity atom, which is responsible for the more powerful interaction. $B_{24}N_{24}$ has the highest positive electrostatic potential, which is in line with the greater propensity of this location for nucleophilic agents. Because oxygen has a lone pair of electrons, it has a tendency to react with the B atom, which has an electron deficiency. Studying the numerical values of the frontier orbitals and E_g for the optimized complexes shows that the LUMO level in complex A is strongly shifted from -0.93 eV to -2.48 eV and -1.52 eV in complex B, Also, E_g in complex A decreases to

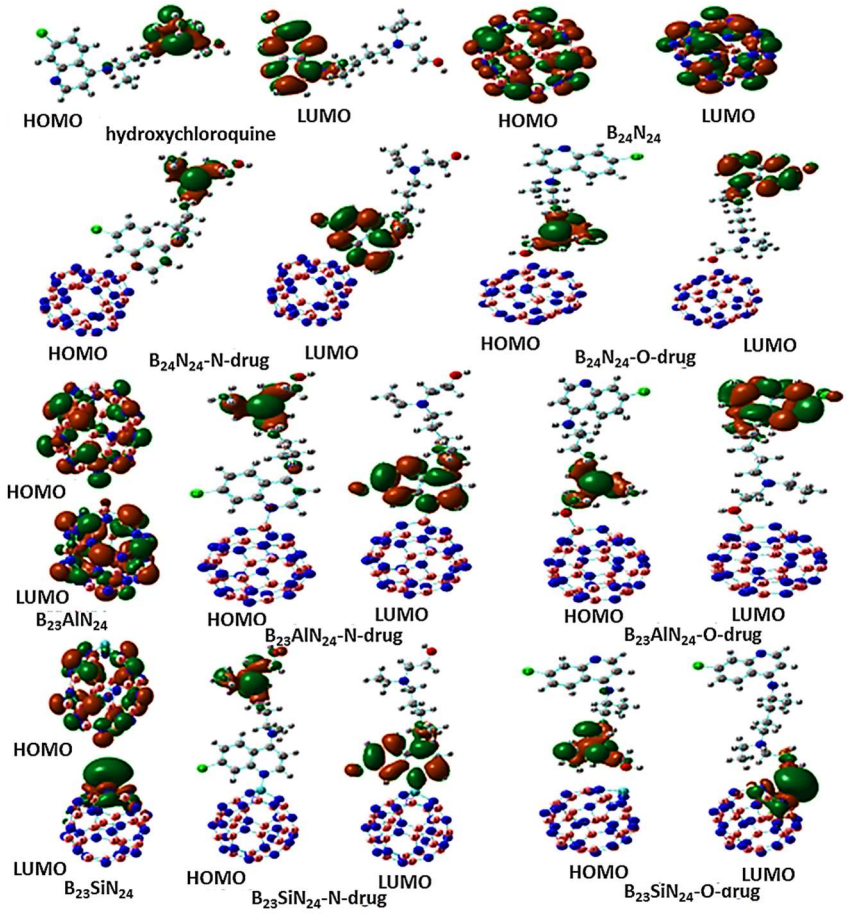

Fig. 4. The HOMO and LUMO profiles for drugs and drug nanocarriers.

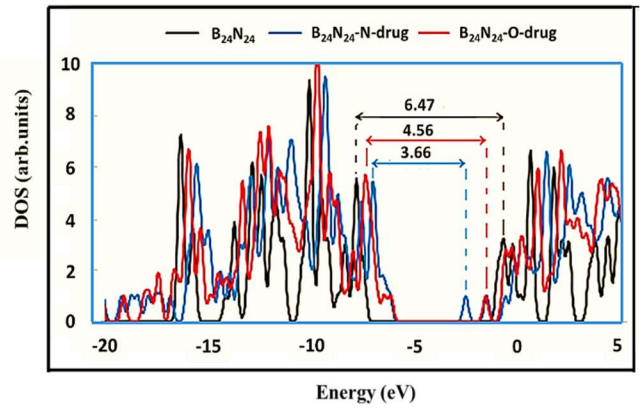

Fig. 5. The DOS plot for $B_{24}N_{24}$, complexes A and B.

3.66 eV and in complex B, E_g changes to 4.56 eV with smaller reduction than in complex A. But after the interaction of the $B_{24}N_{24}$ nanocage with the drug molecule, at the HOMO level, no significant changes were observed. According to the DOS diagram of $AlB_{23}N_{24}$ presented in Fig. 6, it can be understood that the effect of the Al atom on the LUMO levels is greater. When the Al atom in the $B_{24}N_{24}$ cage is doped, the E_g decreases due to the shift in the LUMO level, and this reduction appears after interaction with the drug. In complex C with E_g = 3.66 eV, we have the largest decrease as a result of LUMO shifting to lower values. For complex C in Fig. 4, the shift of LUMO in comparison with the $AlB_{23}N_{24}$ nanocage is evident.

According to the induction of a single electron into Si-doped structures, the molecular orbital (HOMO) is located on the Si atom, and it is used as a factor to calculate E_g. The HOMO and LUMO frontier orbitals for $B_{23}SiN_{24}$ and the stable state of this nanocage with drug, which is complex E, are shown in Fig. 4. According to ESP (Fig. 3), the Si atom is a good place for nuclear nucleophilic attacks due to its

positive charge. Also, Si can donate its lone electron to the drug after nanocage doping E_g is reduced from a value of 6.48 to 4.02 eV. Compared to the bare $B_{24}N_{24}$, Si-doped $B_{24}N_{24}$ nanocages, the LUMO is located on the fullerene after interacting with the drug, and a considerable change exists in HOMO and LUMO levels. The DOS diagram for $B_{23}SiN_{24}$ and complexes E and F in Fig. 7 is a confirmation of the results on the levels of frontier orbitals. Both HOMO and LUMO levels for the E complex are nearly similarly shifted. Chemical potential (μ) is a measure of the tendency of electrons to escape from the system. A high chemical potential difference between the two systems' electron transfer helps. Charge transfer is from a compound that has a higher chemical potential to a compound that has a lower chemical potential. Chemical potential (μ), in recent work for all complexes, is negative in the range of -3.60 to -5.32 eV. According to the data in Table 3, the chemical potential for $B_{23}MN_{24}$ nanocages (M = B, Al, Si) is higher than that of the drug hydroxychloroquine. So it is concluded that we have electron transfer from $B_{23}MN_{24}$ to the drug. So, drug absorption by nanocarrier is well done. The chemical hardness of a molecule indicates its chemical stability. The HOMO-LUMO energy gap can show whether the molecule is hard or soft. Molecules with a high energy gap are known as "hard" and molecules with a low energy gap are known as "soft". As the chemical hardness and energy gap increase, the reactivity decreases. For the $B_{24}N_{24}$ nanocage, after doping and drug absorption by the nanocage from the N atom side of the drug, the chemical hardness decreased.

The total electrophilicity index (ω) is estimated using parameters of electronegativity and chemical hardness. In the conducted research, the value of ω was high for all complexes. As well as, ω was obtained for the $B_{23}SiN_{24}$-O drug more than for other complexes investigated in this research. The particle charge capacity is determined by the parameter ΔN_{max}. According to Eq. (8) of the ΔN_{max} equation, with the increase in chemical potential, we have a decrease in chemical hardness and an increase in electrophilicity. According to the results of Table 3, the value of this parameter in the $B_{23}SiN_{24}$-O-drug complex was higher than that of other complexes. According to the results, the binding of the drug to the nanocages from the O-site.

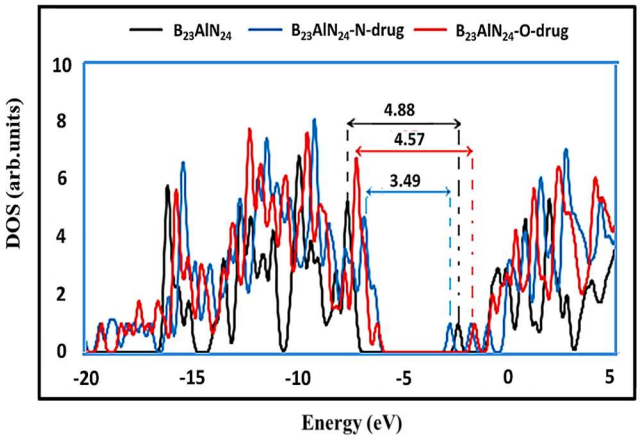

Fig. 6. The DOS plot for $B_{23}AlN_{24}$, complexes C, and D.

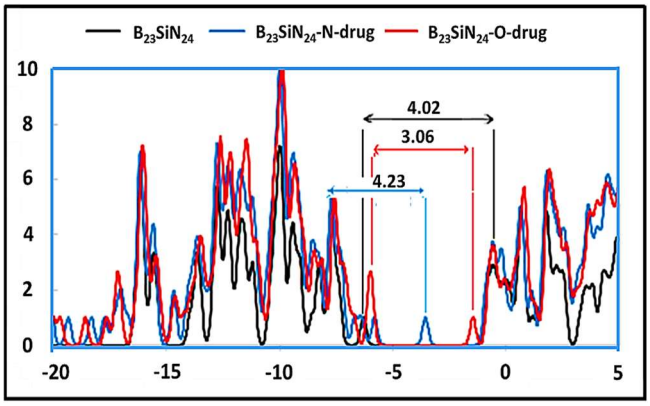

Fig. 7. The DOS plot for $B_{23}SiN_{24}$, complexes E, and F.

Table 1. Interatomic Distance of Drug-Complex and Dipole Moment

Compound	R (Å)	μ (D)
Drug	-	0.07
$B_{24}N_{24}$	-	0.00
$B_{24}N_{24}$-N-Drug	1.645	15.72
$B_{24}N_{24}$-O-Drug	1.708	4.96
$B_{23}AlN_{24}$	-	2.66
$B_{23}AlN_{24}$-N-Drug	1.975	19.42
$B_{23}AlN_{24}$-O-Drug	1.917	8.48
$B_{23}SiN_{24}$	-	0.82
$B_{23}SiN_{24}$-N-Drug	1.748	2.43
$B_{23}SiN_{24}$ -O-Drug	2.722	4.91

Table 2. Absorption Energies for Drug-nanocages

Compound	E_{coh} (kcal mol^{-1})	E_{ad} (kcal mol^{-1})
$B_{24}N_{24}$-N-drug	-150.10	-19.53
$B_{24}N_{24}$-O-drug	-144.33	-10.37
$B_{23}AlN_{24}$-N-drug	-149.51	-49.09
$B_{23}AlN_{24}$-O-drug	149.41	-40.20
$B_{23}SiN_{24}$-N-drug	-149.65	-30.71
$B_{23}SiN_{24}$-O-drug	-149.39	-5.16

E_{coh}: Cohesive energy. E_{ad}: Adsorption energy.

Hydroxychloroquine Drug Release

We know that the pH of target cells is lower than that of healthy cells [42-44]. For this reason, when the drug nanocarrier reaches the target cell, it is possible to be protonated from different points, because the pH of the target cells is lower than that of healthy cells. Due to the ability of N and O atoms to be protonated in an acidic environment, their binding to nanocage in the target cell becomes weaker, so the drug hydroxychloroquine, which has N and O atoms in its structure, has an increased ability for nanocage to act as a drug carrier.

Among other things, the protonation of N in $B_{23}AlN_{24}$-N-drug ($HB_{23}AlN_{24}$-N-drug) increased the Al-N bond length from 1.97 to 2.05 Å (Fig. 8). So, in the target cell, the drug is easily removed from the nanocage. By studying the mechanism of drug release, it can be concluded that as the length of the M-X bond (X = O, N, and M = B, Al, Si) in the investigated nanocage increases, the drug has a greater tendency to be released in the target cells. As a result, we can use this nanocarrier as a drug delivery candidate.

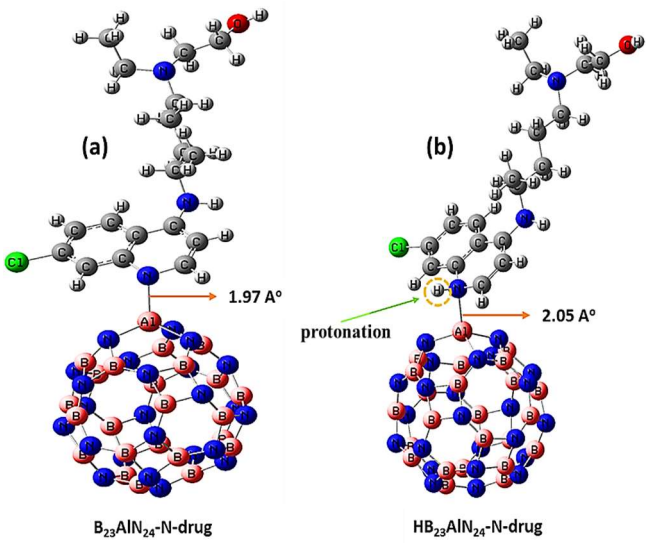

Fig. 8. Structure of (a) $B_{24}N_{24}$Al-N-Hyd, and (b) $HB_{24}N_{24}$Al-N-Hyd.

Table 3. Molecular Orbital Energies and Quantum Descriptors

Compound	E_{HOMO} (eV)	E_{LUMO} (eV)	E_g (eV)	μ (eV)	η (eV)	ω (eV)	ΔN_{max} (eV)	χ (eV)	E_{FL} (eV)
Drug	-5.8218	-1.3826	4.4392	-3.6022	2.2196	2.9230	1.6229	3.6022	-3.6022
$B_{24}N_{24}$	-7.4093	-0.9311	6.4782	-4.1702	3.2391	2.6844	1.2874	4.1702	-4.1702
$B_{24}N_{24}$-N-drug	-6.1479	-2.4838	3.6640	-4.3158	1.8320	5.0835	2.3557	4.3158	-4.3158
$B_{24}N_{24}$-O-drug	-6.0948	-1.5295	4.5652	-3.8121	2.2826	3.1832	1.6700	3.8121	-3.8121
$B_{23}AlN_{24}$	-7.2439	-2.3627	4.8811	-4.8033	2.4405	4.7268	1.9681	4.8033	-4.8033
$B_{23}AlN_{24}$-N-drug	-6.2406	-2.7483	3.4923	-4.4945	1.7461	5.7844	2.5740	4.4945	-4.4945
$B_{23}AlN_{24}$-O-hetro	-6.1690	-1.5973	4.5717	-3.8831	2.2858	3.2982	1.6988	3.8831	-3.8831
$B_{23}SiN_{24}$	-7.3356	-3.3091	4.0264	-5.3224	2.0132	7.0355	2.6437	5.3224	-5.3224
$B_{23}SiN_{24}$-N-drug	-5.8001	-1.5679	4.2321	-3.6840	2.1160	3.2069	1.7410	3.6840	-3.6840
$B_{23}SiN_{24}$-O-drug	-5.9900	-2.9227	3.0673	-4.4563	1.5336	6.4745	2.9057	4.4563	-4.4563

QTAIM Analysis

The AIM molecular graph of the most stable structure of $B_{23}AlN_{24}$-N-Drug was illustrated in Fig. 9; between the nanocage and drug are a number of bond critical points. QTAIM calculations were performed, and the results obtained include electron density (ρ_b) and its Laplacian ($\nabla^2_{\rho_b}$), potential electron energy density (V_b), total electron energy density (H_b), kinetic electron energy density (G_b), and the G_b/V_b ratio, which are presented in Table 4. The value of $\nabla^2_{\rho_b}$ in BCP will be positive when the electronic charge density decreases along the bond path. If the total energy density of the electron ($H_b = G_b+V_b$) is negative, it indicates a shared interaction, and if it is positive, it indicates a closed-shell interaction. Furthermore, the $-G_b/V_b > 1$ is used to determine noncovalent interactions and $-G_b/V_b < 1$ when the interaction is covalent [45,46]. The calculations indicate that for $B_{23}AlN_{24}$-N-Drug bonds of the Al-N, $\nabla 2\rho b > 0$, $H_b > 0$, and $-G_b/V_b < 1$, which means interactions between drug and na nocage have a "closed-shell" noncovalent nature.

Practical Limitations

There are some limitations in using boron nitride nanocages as drug carriers in biological environments. One of these constraints is economic limitations in mass production, and another constraint is clinical, which must be considered during clinical work. More extensive research in this area needs to be conducted to determine under what conditions the body's acidic and alkaline environments impose the highest-burden and controlled release of drugs [8,9].

Table 4. The Electron Density (ρ_b), Laplacian of Electron Density ($\nabla^2_{\rho_b}$), Kinetic Electron Energy Density (G_b), Potential Electron Energy Density (V_b), Total Electron Energy Density (H_b), and $-G_b/V_b$ Ratio at the Bond Critical Points (BCPs) of the Studied Complexes. All the Values are in au

System	ρ_b	$\nabla^2_{\rho_b}$	G_b	V_b	H_b	$-G_b/V_b$
$B_{23}AlN_{24}$-N-drug	0.0608	0.0840	0.0851	-0.0850	0.1705	1.0011

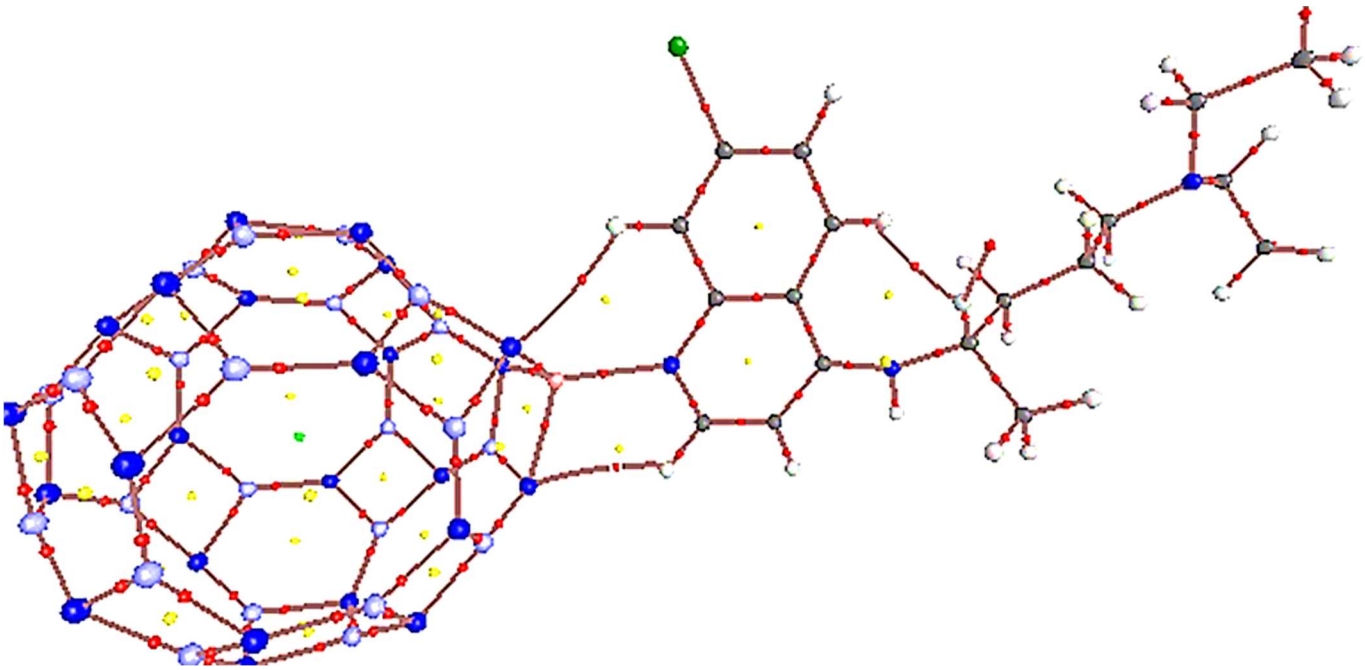

Fig. 9. The molecular graphs of the studied complexes obtained by QTAIM analysis.

CONCLUSIONS

In the present work, we have performed DFT calculations to study the interactions between the $B_{24}N_{24}$ nanocage and the Al, Si-doped nanocage with the hydroxychloroquine drug. It is found that the $B_{24}N_{24}$ nanocage, due to poor interaction and an E_{ad} of approx. 10.07 kcal mol^{-1} for $B_{24}N_{24}$-O-drug and -19.53 kcal mol^{-1} for $B_{24}N_{24}$-N-drug, cannot be considered a suitable carrier for the hydroxychloroquine drug. Furthermore, to improve adsorption, a B atom of the nanocage is replaced by Si or Al atoms. The results showed that the E_{ad} with Al and Si-doped increases to -40.20 for $B_{23}AlN_{24}$-O-drug, -49.09 kcal mol^{-1} for $B_{23}AlN_{24}$-N-drug, and -30.71 for $B_{23}SiN_{24}$-N-drug, respectively. The most stable configuration is an Al-doped $B_{24}N_{24}$ nanocage, releasing energy of about -49.09 kcal mol^{-1}. AIM calculations with results including, $H_b > 0$, and $-G_b/V_b < 1$ showed interactions between drug and nanocage have a "closed-shell" non-covalent nature. The E_g for these systems has slightly decreased. For the $AlB_{23}N_{24}$, E_g is reduced from 4.88 to 3.49 eV . It was shown that when the PH of the tissues is low, the drug can be released by a proton attack from the nanocage. The drug release from the system was checked by checking the $B_{23}AlN_{24}$-N-drug protonation of the N atom in the $B_{23}AlN_{24}$-N-drug. ($HB_{23}AlN_{24}$-N-drug) increased the Al-N bond from 1.975 to 2.054 Å (Fig. 8). It can be concluded that the drug in the target cell, is easily removed from the nanocage.

ACKNOWLEDGMENT

The authors express their appreciation to the post-graduate office of Ayatollah Alozma Borujerdi University for the financial support of this work.

REFERENCES

[1] Chen, Z., *et al.* Efficacy of hydroxychloroquine in patients with COVID-19: results of a randomized clinical trial. *medRxiv*, **2020**. DOI: https://doi.org/10.1101/2020.03.22.20040758.

[2] Chen, J., *et al.* A pilot study of hydroxychloroquine in treatment of patients with common coronavirus disease-19 (COVID-19). *J. Zhejiang Univ. (Med. Sci.).* **2020**, *49*, DOI: 10.3785/j.issn.1008-9292.2020.03.03.

[3] Kumar Singh, A.; Singh, A.; Singh, R.; Misra, A., Hydroxychloroquine in patients with COVID-19: A Systematic Review and meta-analysis. Diabetes & Metabolic Syndrome: *Clinical Research & Reviews*, **2020**, *14*, 589-596, DOI: 10.1016/j.dsx.2020.05.017.

[4] Cavalcanti Iago, D. L.; Ramos dos Santos Medeiros, F.; Sandrelli, M., dos Santos, M.; Charles, M.; Cavalcanti, F.; Macário, I.; Nogueira, B. L.; Cajubá, M., Nanocarriers in the Delivery of Hydroxychloroquine to the Respiratory System: An Alternative to COVID-19. *Curr. Drug Delivery*. **2021**, *18*, 583-595, DOI: 10.2174/1567201817666200827110445.

[5] Kadhum, S. T.; Alkindi, G. Y.; Albayati, T. M., Remediation of phenolic wastewater implementing nano zerovalent iron as a granular third electrode in an electrochemical reactor. *International Journal of Environmental Science and Technology*. **2022**, *19*, 1383-1392, https://doi.org/10.1007/s13762-021-03205-5.

[6] Najibzade, Y.; Sheikhhosseini, E.; Akhgar, M. R.; Ahmadi, S. A., Absorption of tranylcypramine on C_{60} nanocage: Thermodynamic and electronic properties. *Pakistan Journal of Pharmaceutical Sciences.* **2022**, *35*, 815-818, doi.org/10.36721/PJPS.2022.35.3.REG.815-818.1.

[7] Nazarali, Z.; Ahmadi, S. A.; Ghazanfari, D.; Sheikhhosseini, E.; Razavi, R., Investigation of Flutamide@ethyleneimine as Drug Carrier by Nanocone and Nanotube Theoritically, *Iran. J. Chem. Chem. Eng. (IJCCE), In press*. Doi: 10.30492/ijcce.2021.542408.5014.

[8] H. F.; Alazzawi, I. K.; Salih, Albayati, T. M., Drug delivery of amoxicillin molecule as a suggested treatment for covid-19 implementing functionalized mesoporous SBA-15 with aminopropyl groups. *Drug Delivery*, **2021**, *28* (1) 856-864, https://doi.org/10.1080/10717544.2021.1914778.

[9] Fekri, M. H.; Soleymani, S.; Razavi Mehr, M.; Akbari-adergani, B., Synthesis and characterization of mesoporous ZnO/SBA-16 nanocomposite: its efficiency as drug delivery system, *Journal of Non-Crystalline Solids*, **2022**, *591*, 121512, https://doi.org/10.1016/j.jnoncrysol. 2022.121512.

[10] Tavakoli, H.; Ahmadi, S. A.; Ghazanfari, D.; Sheikhhosseini, E., Theoretical investigation of functionalized fullerene nano carrier drug delivery of fluoxetine. *Journal of the Indian Chemical Society*. **2022**, *99*, 100561, https://doi.org/10.1016/j.jics.2022.100561.

[11] Rahimi, R.; Solimannejad**,** M., A novel pentagonal BCN monolayer for sensing and drug delivery of nitrosourea and hydroxyurea anticancer drugs: A DFT outlook. *Materials Science in Semiconductor Processing*. **2024**, *173*, 108109. ttps://doi.org/10.1016/j.mssp.2024.108109.

[12] Rahimi, R.; Solimannejad, M., *In silico* study of B_3O_3 nanosheet as a disposable platform for sensing and delivery of carmustine anticancer drug. *Journal of Drug Delivery Science. and Technology* **2023**, *87*, 104828, https://doi.org/10.1016/j.jddst.2023.104828.

[13] Rahimi, R.; Solimannejad, M., B_3O_3 monolayer with dual application in sensing of COVID-19 biomarkers and drug delivery for treatment purposes: A periodic DFT study, *J. Mol. Liq*. **2022**, *354*, 118855, https://doi.org/10.1016/j.molliq.2022.118855.

[14] Rahimi, R.; Solimannejad, M.; Solimannejad, M., Two-dimensionalcovalent triazine frameworks as superior nanocarriers for the delivery of thioguanine anti-cancer drugs: a periodic DFT study. *New Journal of Chemistry*. **2022**, *46*, 15635-15644, https://doi.org/10.1039/D2NJ02050.

[15] Rahimi, R.; Solimannejad, M.; Ehsanfar, Z., First-principles studies on two-dimensional B_3O_3 adsorbent as a potential drug delivery platform for TEPA anticancer drug. *J. Mol. Model*. **2021**, *27*, 1-10, https://doi.org/10.1007/s00894-021-04930-x.

[16] Rahimi, R.; Solimannejad, M.; Farghadani, M., Adsorption of chloroquine and hydroxychloroquine as potential drugs for SARS-CoV-2 infection on BC_3 nanosheets: a DFT study. *New J. Chem*. **2021**, *45*, 17976-17983, https://doi.org/10.1039/D1NJ03084A.

[17] Rahimi, R., Solimannejad, M., BC_3 graphene-like monolayer as a drug delivery system for nitrosourea anticancer drug: A first-principles perception. *Appl. Surf. Sci*. **2020**, *525*, 146577, https://doi.org/10.1016/j.apsusc.2020.146577.

[18] Rahimi, R.; Solimannejad, M.; Ehsanfar, Z., Potential application of XC3 (X = B, N) nanosheets in drug delivery of hydroxyurea anticancer drug: a comparative DFT study, *Mol. Phys*. **2022**, *120*, e2014587, https://doi.org/10.1080/00268976.2021.2014587.

[19] Xu, H.; Wang, Q.; Fan, G.; Chu, X., Theoretical study of boron nitride nanotubes as drug delivery vehicles of some anticancer drugs, *Theor. Chem. Accounts* **2018**, *137*, 104. DOI: 10.1007/s00214-018-2284-2.

[20] Xu, H.; Li, L.; Fan, G.; Chu, X., DFT study of nanotubes as the drug delivery vehicles of Efavirenz. *Comput. Theor. Chem*. **2018**, *1131*, 57-68, DOI: 10.1016/J.COMPTC.2018.03.032.

[21] Ammar, H. Y.; Eid, K. M.; Badran, H. M., TM-doped $Mg_{12}O_{12}$ nano-cages for hydrogen storage applications: Theoretical study. *Results in Physics*. **2022**, *35*, 105349, https://doi.org/10.1016/j.rinp.2022.105349.

[22] Xu, H.; Tu, X.; Fan, G.; Wang, Q.; Wang, X.; Chu, X., Adsorption properties study of boron nitride fullerene for the application as smart drug delivery agent of the anti-cancer drug hydroxyurea by density functional theory. *J. Mol. Liq*. **2020**, *318*, 114315, DOI: 10.1016/j.molliq.2020.114315.

[23] Golipour-Chobar, E.; Salimi, F.; Ebrahimzadeh Rajaei, G., Boron nitride nanocluster as a carrier for lomustine anticancer drug delivery: DFT and thermodynamics studies. *Monatsh. Chem*. **2020**, *151*, 309-318, DOI: 10.1007/s00706-020-02564-y.

[24] Khodam Hazrati, M.; Javanshir, Z.; Bagheri Z., $B_{24}N_{24}$ fullerene as a carrier for 5-fluorouracil anti-cancer drug delivery: DFT studies. *J. Mol. Graphics Model*. **2017**, *77*, 17-24, DOI: 10.1016/j.jmgm.2017.08.003.

[25] Padasha, R.; Rabbani Esfahanib A., Shokuhi Radc, The computational quantum mechanical study of sulfamide drug adsorption onto $X_{12}Y_{12}$ fullerene-like nanocages: detailed DFT and QTAIM investigations. *J. Biomol. Struct. Dyn*. **2021**, *39*, 5427-5437, DOI: 10.1080/07391102.2020.1792991.

[26] El-Mageed, H. R.; Mustafa, F. M.; Abdel-Latif, K., Mahmoud, Boron nitride nanoclusters, nanoparticles, and nanotubes as a drug carrier for isoniazid anti-tuberculosis drug, computational chemistry approaches. *J. Biomol. Struct. Dyn*. **2020**, 1-10*,* https://doi.org/10.1080/07391102.2020.1814871.

[27] Oku, T.; Nishiwaki, A.; Narita, I.; Gonda, M., Formation and structure of $B_{24}N_{24}$ clusters. Chem. *Phys. Lett*. **2003**, *380*, 620-623, https://doi.org/10.1016/j.cplett.2003.08.096.

[28] Chen, X.; Wu, P.; Rousseas, M.; Okawa, D.; Gartner, Z.; Zettl, A.; Bertozzi, C. R., Boronnitride nanotubes are noncytotoxic and can Be functionalized for interactionwith proteins and cells. *J. Am. Chem. Soc*. **2009**, *131*, 890-891, https://doi.org/10.1021/ja807334b.

[29] Gholami, R.; Solimannejad, M., nanocluster for sensing and delivering aloe-emodin anticancer drug: A DFT study. *Journal of Molecular Structure*. **2022**, *1270*, 133968, https://doi.org/10.1016/j.molstruc.2022.133968.

[30] Frisch, M. J.; Trucks, G. W.; Schlegel, H. B.; Scuseria, G. E.; Robb, M. A.; Cheeseman, J. R.; Scalmani, G.; Barone, V.; Mennucci, B.; Petersson, G. A.; Nakatsuji, H.; Caricato, M.; Li, X.; Hratchian, H. P.; Izmaylov, A. F.; Bloino, J.; Zheng, G.; Sonnenberg, J. L.; Hada, M.; Ehara, M.; Toyota, K.; Fukuda, R.; Hasegawa, J.; Ishida, M.; Nakajima, T.; Honda, Y.; Kitao, O.; Nakai, H.; Vreven, T.; Montgomery, J. J.; Peralta, J. E.; Ogliaro, F.; Bearpark, M.; Heyd, J. J.; Brothers, E.; Kudin, K. N.; Staroverov, V. N.; Kobayashi, R.; Normand, J.; Raghavachari, K.; Rendell, A.; Burant, J. C.; Iyengar, S. S.; Tomasi, J.; Cossi, M.; Rega, N.; Millam, J. M.; Klene, M.; Knox, J. E.; Cross, J. B.; Bakken, V.; Adamo, C.; Jaramillo, J.; Gomperts, R.; Stratmann, R. E.; Yazyev, O.; Austin, A. J.; Cammi, R.; Pomelli, C.; Ochterski, J. W.; Martin, R. L.; Morokuma, K.; Zakrzewski, V. G.; Voth, G. A.; Salvador, P.; Dannenberg, J. J.; Dapprich, S.; Daniels, A. D.; Farkas, O.; Foresman, J. B.; Ortiz, J. V.; Cioslowski, J.; Fox, J., GAUSSIAN 09, Revision A.1, GAUSSIAN Inc., Wallingford, CT., **2009**.

[31] Fekri, M. H.; Eskandari, F.; Razavi Mehr, M.; Banimahd Keyvani, M.; Habibi, N., Investigations of solvent effect on electrochemical and electronically properties of some quinone drugs: a computational study, *Iran. J. Math. Chem*. **2022**, *13*, 187-199, DOI: 10.22052/IJMC.2022.246300.1621.

[32] Fekri, M. H.; Beyranvand, A.; Dashti Khavidaki, H.; Razavi Mehr, M., Cycloaddition [2+2] interaction of some corticosteroid drugs with C_{60} nano fullerene-A theoretical study. *Int. J. Nano Dimens*. **2021**, *12*, 156-163, DOI: 20.1001.1.20088868.2021.12.2.8.5.

[33] Fekri, M. H.; Bazvand, R.; Solymani, M.; Razavi Mehr, M., Adsorption behavior, electronical and thermodynamic properties of ornidazole drug interaction with C_{60} fullerene doped with Si, B and Al: A quantum mechanical simulation. *Phys. Chem. Res*. **2021**, *9*, 151-164, DOI: 10.22036/pcr.2020.244279.1814.

[34] Ghasemi, A. S.; Ramezani Taghartapeh, M.; Soltani, A.; Mahon, P. J., Adsorption behavior of metformin drug on boron nitride fullerenes: Thermodynamics and DFT studies. *J. Mol. Liq*. **2019**, *275*, 955-967, DOI: https://doi.org/10.1016/j.molliq.2018.11.124.

[35] O'boyle, N. M.; Tenderholt, A. L.; Langner, K. M., A library for package-independent computational chemistry algorithms. *J. Comput. Chem*. **2008**, *29*, 839-845, https://doi.org/10. 1002/jcc.20823.

[36] Keith, T. A., AIMAll (Version 10.07. 25). Overland Park, KS, USA: TK Gristmill Software **2010**.

[37] Parlak, C.; Alver, O., A density functional theory investigation on amantadine drug interaction with pristine and B, Al, Si, Ga, Ge doped C_{60} fullerenes. *Chem. Phys. Lett*. **2017**, *678*, 85-90, DOI: 10.1016/j.cplett.2017.04.025.

[38] Hazrati, H. K.; Hadipour, L. N., Adsorption behavior of 5-fluorouracil on pristine, B-, Si, and Al-doped C_{60} fullerenes: A first principles study. *Phys. Lett. A* **2016**, *380*, 937-941, DOI: 10.1016/j.physleta.2016.01.020.

[39] Bashiri, S.; Vessally, E.; Bekhradnia, A.; Hosseinian, A.; Edjlali, L., Utility of extrinsic [60] fullerenes as work function type sensors for amphetamine drug detection: DFT studies. *Vacuum*. **2017**, *136*, 156-162, https://doi.org/10.1016/j.vacuum.2016.12.003.

[40] Fekri, M. H.; Bazvand, R.; Solymani, M.; Razavi Mehr, M., Adsorption of Metronidazole drug on the surface of nano fullerene C_{60} doped with Si, B and Al: A DFT Study. *Int. J. Nano Dimens*. **2020**, *11*, 346-354, DOI: 20.1001.1.20088868.2020.11.4.4.8.

[41] Hazrati, M. K.; Bagheri, Z.; Bodaghi, A., Application of $C_{30}B_{15}N_{15}$ heterofullerene in the isoniazid drug delivery: DFT studies. *Physica E.* **2017**, *89*, 72-76, DOI: 10.1016/.physe.2017.02.009.

[42] Hazrati, M. K.; Bagheri, Z.; Bodaghi, A., Application of $C_{30}B_{15}N_{15}$ heterofullerene in the isoniazid drug delivery: DFT studies. *Physica E.* **2017**, *89*, 72-76, DOI: 10.1016/.physe.2017.02.009.

[43] Nagarajan, V.; Chandiramouli, R., A study on quercetin and 5-fluorouracil drug interaction on graphyne nanosheets and solvent effects-A firstprinciples study. *J. Mol. Liq*. **2018**, *275*, 713-722, DOI: 10.1016/ j.molliq.2018.11.083.

[44] Srimathi, U.; Nagarajan, V.; Chandiramouli, R. V., Interaction of imuran, pentasa and hyoscyamine drugs and solvent effects on graphdiyne nanotube as a drug delivery system-A DFT study. *J. Mol. Liq.* **2018**, *265*, 199-207, DOI: 10.1016/ j.molliq. 2018.05.114.

[45] Cremer, D.; Kraka, E., Chemical bonds without bonding electron density-does the difference electron-density analysis suffice for a description of the chemical bond? *Angew. Chem. Int. Ed. Engl.* **1984**, *23*, 627-628.

[46] Mohajeri, A.; Alipour, M.; Mousaee, M., Halogen-hydride interaction between Z−X (Z = CN, NC; X = F, Cl, Br) and H−Mg−Y (Y = H, F, Cl, Br, CH_3). *J. Phys. Chem. A* **2011**, *115*, 4457-4466, https://doi.org/10.1021/jp200689b.